In quest of the optimal coincidence resolving time in TDCR LSC

Chavdar Dutsov, Philippe Cassette, Krasimir Mitev, Benoît Sabot

In quest of the optimal coincidence resolving time in TDCR LSC

Chavdar Dutsov[a,*], Philippe Cassette[a], Krasimir Mitev[a], Benoît Sabot[b]

[a] *Sofia University "St. Kliment Ohridski", Faculty of Physics, 5 James Bourchier Blvd, 1164 Bulgaria*
[b] *CEA, LIST, Laboratoire National Henri Becquerel, LNE-LNHB, 91191, Gif- sur-Yvette Cedex, France*

Abstract

This paper presents studies of the influence of the coincidence resolving time on the activity calculated by the Triple-to-Double Coincidences Ratio (TDCR) method in Liquid Scintillation (LS) counting. Recently, published methods for the correction for accidental coincidences in TDCR counting open the possibility to use resolving times up to several µs, long enough not to miss true coincidences and to study the effects of delayed fluorescence.

^{3}H, ^{14}C, ^{55}Fe and ^{63}Ni LS-sources in UltimaGold (UG), UG LLT and Toluene+PPO cocktails were measured using a TDCR counter connected to a digitizer working in list-mode. The necessary resolving time to include 99.9% of the logical sum of double (D) coincidences was found to be 1.2 µs for ^{3}H, 1 µs for ^{55}Fe and 500 ns for ^{63}Ni in UG. The activity of all LS-sources was calculated using the TDCR method for resolving times from 10 ns to 2 µs and a significant dependence between the calculated activity and resolving time was observed. A dedicated Monte Carlo (MC) code was used to simulate list-mode data from TDCR measurements. The simulation results suggest that the ^{3}H activity calculated by the TDCR method is overestimated regardless of the used resolving time if delayed fluorescence is present which is not described by the used ionization quenching function.

Efficiency variation measurements of ^{3}H in UG LLT show a strong dependence of the optimal kB parameter on the used resolving time: 85 µm/MeV at 40 ns and 110 µm/MeV at 200 ns, leading to 2.5% difference in calculated activity. In the framework of this study the efficiency variation methods by chemical quenching and gray filters were compared and a difference of 60 µm/MeV between the two was observed.

The results from this article demonstrate that regardless of the available corrections for accidental coincidences, it is not advisable to increase the resolving time beyond what is necessary to register all prompt fluorescence events. Moreover, even for short coincidence resolving times, delayed fluorescence could have a significant influence on the activities calculated by the TDCR method.

Keywords: TDCR, Delayed fluorescence, LSC, Coincidence resolving time

1. Introduction

The TDCR method is widely used for the standardization of pure β-emitting and some electron-capture radionuclides [1] by Liquid Scintillation Counting techniques (LSC). The application of the method requires a specialized LS analyzer with three photomultiplier tubes (PMTs) and electronics capable of counting coincidences between three PMTs as well as between pairs of PMTs. For two or three events to be considered in a double or triple coincidence, respectively, the time difference between the events must be shorter than a predefined time referred to as coincidence resolving time or coincidence window.

The TDCR method uses the ratios of the triple coincidences to each of the double coincidences to calculate the detection efficiency [2]. If the used coincidence resolving time is too short some coincidences will be missed and this may lead to a bias in the efficiency and activity calculated by the method. It

*Corresponding author
Email address: ch.dutsov@phys.uni-sofia.bg (Chavdar Dutsov)

Table 1: Composition of the studied sources. The vial type of PE refers to Polyethylene vials and G + DT to borosilicate glass vial wrapped with a layer of diffusive tape. The given detection efficiency ε_D is for the logical sum of double coincidences. The final column contains the approximate mass of the aqueous solution ($m_{\mathrm{H_2O}}$) and the total mass of the scintillation cocktail (m_{tot})

.

Source name	Nuclide	Avg. TDCR	ε_D	Activity, Bq	LS cocktail	Vial type	$m_{\mathrm{H_2O}}/m_{\mathrm{tot}}$, g
H3-UG	^{3}H	0.399	0.43	23 000	UG	PE	0.1 / 10
H3-LLT	^{3}H	0.435	0.47	3070	UG LLT	PE	0.1 / 10
H3-Tol	^{3}H	0.582	0.64	470	Tol. + PPO	G + DT	0.0 / 10
H3-UGQ (1–7)	^{3}H	0.4–0.2	0.44–0.18	2600	UG	PE	0.1 / 10
Fe55-UG	^{55}Fe	0.280	0.48	13 300	UG	PE	0.1 / 10
Fe55-HF	^{55}Fe	0.185	0.31	13 700	HF	PE	0.1 / 10
Ni63-UG	^{63}Ni	0.760	0.75	1100	UG	G + DT	0.1 / 10
C14-UG	^{14}C	0.931	0.94	6300	UG	G + DT	0.1 / 10

has been observed that for the high-energy emitter ^{18}F ($E_{\beta\mathrm{max}}$ 633 keV) the first detected events in each PMT are grouped within 16 ns. For ^{3}H ($E_{\beta\mathrm{max}}$ 18.6 keV) the spread of events is much larger, with reports up to 250 ns [3] and above 300 ns [4]. A study of the scintillation intensity dependence with time of the commonly used solvent/flour combination diisopropylnaphtalene (DIN) and 2,5-diphenyloxyzole (POP) reports scintillation events up to 1.5 µs [5]. Such large time spread of events would seem to require the use of much wider coincidence windows than the ones currently in use, between 20 and 200 ns, with 40 ns being the resolving time of the commonly used MAC3 acquisition module [6].

There are mainly two types of luminescence which can occur in organic molecules: fluorescence and delayed fluorescence. Fluorescence, sometimes refered to as prompt fluorescence, is a result of radiative transitions from singlet S_1 to S_0 states of the solvent and its intensity decays exponentially with time with lifetimes in the order of few nanoseconds [7]. Delayed fluorescence decays occur within a few µs after the excitation of the solvent and is due to triplet-triplet interactions resulting in S_1 excitations, for example $T_1 + T_1 \rightarrow S_1 + S_0$ [7].

Previous studies of the influence of the coincidence resolving time on the activity calculated by the TDCR method can be found in the literature, but the maximum studied resolving time is usually in the order of few hundred nanoseconds, without corrections for accidental coincidences. For example, in one study of ^{3}H in Insta-Gel [8] the largest resolving time studied is 200 ns and in another study of ^{3}H in HionicFluor (HF) and UG cocktails [9], coincidence windows up to 400 ns were analyzed. Such resolving times should be enough to gather all events due to prompt fluorescence, but could be insufficient to include the events from delayed fluorescence which could have a non-negligible influence to the overall light emission [7].

With advances in digital electronics, an increase in the number of custom-made TDCR acquisition systems can be seen, all having the possibility to use arbitrary long resolving times [3, 10, 11, 12, 13]. Moreover, a method for correcting for accidental coincidences was presented in a recent paper [14]. These conditions give the opportunity to expand the resolving time to be long enough to register all scintillation events, including delayed fluorescence. Care must be taken, however, because delayed fluorescence could have different ionization quenching properties than prompt fluorescence, which is the only type of fluorescence considered in Birks' ionization quenching formula [7]. The TDCR model has been shown to be very sensitive to the parameters used to describe the ionization quenching for low-energy β emitters like ^{3}H [15].

The objective of the present work is to study the dependence of the measured counting rate and calculated activity on the used coincidence resolving time, using long enough coincidence windows to include all correlated scintillation events. One novel approach of the presented study is the correction of the coincidence counting rates for accidental coincidences, which have non-negligible effect in the case of long resolving times.

2. Materials and methods

Experimental setup. In order to study the distribution of the light emission in time of various LS-sources a portable 3D-printed TDCR counter has been used. The counter, referred to as the *miniTDCR*, was developed at the *Laboratoire National Henri Becquerel*. One important feature of the used counter is an optical filter holder that ensures that the measurement geometry is kept constant between measurements. The counter was connected to a CAEN DT5751 desktop digitizer [16] with four channels and 1 GS/s sampling rate per channel. Each of the three PMTs of the TDCR counter are connected to a channel of the digitizer which records a time stamp with 1 ns resolution of each incoming event into *list-mode* files for off-line processing, one file per connected channel. The list-mode files were processed with a dedicated home-made software (hereafter referred to as `TDCR_analysis`) written in the Rust programming language, which is a strongly-typed systems programming language with similar syntax and performance as C++, but has the advantage of being memory safe without using garbage collection. A major advantage of this experimental setup is that the counting rate in all coincidence channels and for arbitrarily long resolving times can be obtained from a single measurement, thus eliminating possible effects due to counting uncertainties. In one experiment the results obtained with this system were compared to results obtained with the French primary TDCR counter RCTD1 [17] equipped with three Burle 8850 PMTs connected to a nanoTDCR device [10] after an amplifier and a discriminator.

In the current work, measurements of seven LS-sources and the corresponding blank samples were performed. The composition of the studied sources is presented in Table 1Composition of the studied sources. The vial type of PE refers to Polyethylene vials and G + DT to borosilicate glass vial wrapped with a layer of diffusive tape. The given detection efficiency ε_D is for the logical sum of double coincidences. The final column contains the approximate mass of the aqueous solution ($m_{\mathrm{H_2O}}$) and the total mass of the scintillation cocktail (m_{tot})table.1. The ^{3}H and ^{63}Ni sources were measured with a set of home-made optical gray filters in order to perform the efficiency variation method, used in TDCR measurements for the determination of the optimal kB parameter. The H3-UGQ sources are a set of seven 10 ml UG cocktail LS-sources with added nitromethane with weight from 0 mg to 70 mg.

Analysis of the list-mode files. For each measurement with the digitizer, a set of three files with the time-stamp of each recorded event (one file for each PMT channel) is produced. The `TDCR_analysis` program opens the list-mode files and applies the common-dead time logic (used in the MAC3 module [6]). Whenever an event is registered in a given channel, a common dead-time for all three channels will be triggered and a common coincidence window will be opened. Only the first registered event in a given channel (primary event) is considered and other events in the same channel are ignored for the duration of the coincidence window. The timestamps of the primary events, relative to the start of the coincidence window are recorded and can be used to construct the time difference spectra of the time differences Δt_i for each coincidence channel $i = AB, BC, AC, D$ or T. The `TDCR_analysis` code works as follows:

The first incoming event opens a common coincidence window and sets a timestamp for the start of the dead-time. For the duration of the coincidence window, only the first incoming event in a given channel is registered. This is done in order to consider only real events and not afterpulses.

At the end of the coincidence resolving time, the coincidence counters are incremented appropriately and the histogram $h^{(i)}$ for the selected by the user time distribution is incremented. If the time distribution for the D channel is required and there is a D event during the coincidence resolving time, the histogram bin corresponding to a time difference Δt between the second and the first arriving primary events is recorded. If the selected time distribution is for the T channel, the histogram bin corresponding to the time difference between the third and first arriving primary events is recorded, only if there is a triple coincidence during the coincidence resolving time.

If the selected time distribution is for one of the double coincidence channels AB, BC or AC, it must be noted that some of these events are also T events. If there is a double coincidence from the requested type and there is no T coincidence during the coincidence resolving time, the time difference that is recorded in the histogram is the time between the secondary and reference channels. If there is a T coincidence during

the coincidence resolving time, the recorded time difference will be that of the T event. A graphic depiction of the same logic used for the calculation of the different Δt_i can be seen in [14].

After the analysis of all files is completed, the `TDCR_analysis` code outputs the histogram of the time differences for the user-selected coincidence channel. The histogram has a bin width $b = 1$ ns. The time differences Δt_i described above are defined in such a way that the histograms $h^{(i)}$ fulfill the following criteria:

$$n^{(i)}(\tau) = \frac{1}{L}\sum_{t=0}^{\tau/b} h_t^{(i)}, \tag{1}$$

where $n^{(i)}$ is the counting rate that would be reported by a TDCR measurement with coincidence resolving time τ and live-time L. The histograms $h^{(i)}$ give the opportunity to study the counting rate for a given channel as a function of the coincidence resolving time with a single measurement.

Correction for accidental coincidences. In order to obtain the time distribution of the true coincidences a correction for accidental coincidences is necessary. The method for correction for accidental coincidences is described in detail in [14]. It is based on the analysis of the time distribution in a given coincidence channel. The underlying assumption is that coincidences of primary events separated by several microseconds in time are accidental. By analyzing the time distribution in the region where the rate of occurrence of true coincidences is negligible, the contribution of the accidental coincidences can be estimated. The measured time distribution $f_i(t)$ is the sum of the distribution of true events $f_{\text{true}}(t)$ and the distribution of the accidental coincidences. As the accidental coincidences are formed by uncorrelated events and if their occurrence is a Poissonian process, then their distribution in time is exponential, which gives:

$$f(t) = f_{\text{true}}(t) + a_0 e^{-\lambda t}, \tag{2}$$

where a_0 are the accidental coincidences at time zero and λ is the rate of coincidence events. For the counting rates measured in this study, the argument of the exponent is less than 10^{-2} and the distribution of the accidental coincidences can be approximated with a linear function. The parameters of the distribution can then be determined by a linear fit in the region where the contribution of the true coincidences can be assumed negligible. The contribution of the accidental coincidences in the ith channel in a given bin can then be calculated as:

$$a_t^{(i)} = a_0 - a_1 t. \tag{3}$$

where a_0 and a_1 are the parameters of the linear fit of the time interval distribution. In this study the fit was performed using time distribution data between 2 µs and 3 µs. This interval was found to contain negligible contribution from true coincidences and is short enough to approximate the exponential distribution of the accidental coincidences with a linear function.

The counting rate of the true coincidence in a given coincidence channel i can then be determined as:

$$n_{\text{true}}^{(i)}(\tau) = \frac{1}{L}\sum_{t=0}^{\tau/b}\left[h_t^{(i)} - a_t^{(i)}\right]. \tag{4}$$

The dependence of the measured $n^{(i)}$ and the corrected for accidental coincidences $n_{\text{true}}^{(i)}$ counting rates with respect to the coincidence resolving time for the H3-UG source is shown in Figure 1Counting rate in the D channel of the H3-UG measurement relative to the counting rate at 2 µs coincidence resolving time with and without correction. The dashed line shows the fit of the corrected relative counting rate after 2 µsfigure.1. After correcting for accidental coincidences, the counting rate is not dependent on the resolving time, after the time needed to collect all true coincidences. The dashed line shows the linear fit of the function. The slope of the corrected counting rate is less than 2×10^{-8} ns^{-1} or 2×10^{-5}% increase in the counting rate for every 1000 ns coincidence resolving time.

The correction for accidental coincidences was performed on all measurements discussed in this paper, including blank measurements, using the `TDCR_analysis` program. The accidental coincidences are assumed to be all coincidences with time difference larger than 2 µs and the parameters of the accidental coincidences distribution were obtained by linear fit of the time distribution histogram between 2 µs and 3 µs.

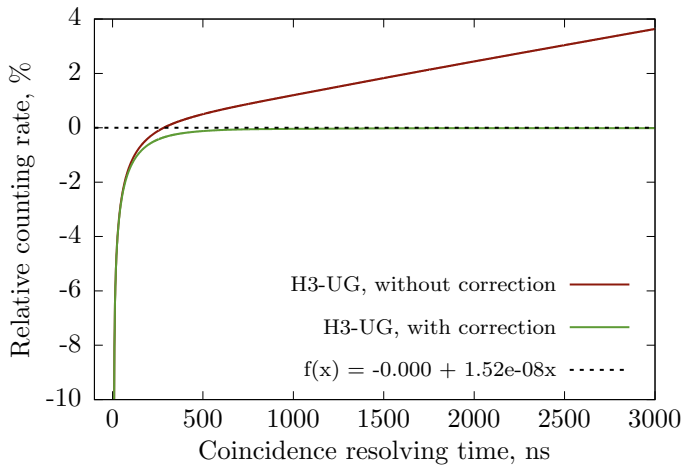

Figure 1: Counting rate in the D channel of the H3-UG measurement relative to the counting rate at 2 µs coincidence resolving time with and without correction. The dashed line shows the fit of the corrected relative counting rate after 2 µs.

MC code for the simulation of the timing of TDCR events. To gain a better understanding of the influence which the delayed fluorescence could have on activity calculations with the TDCR method, we have developed a dedicated MC code for the simulation of the timing of events in TDCR counting. The code was written in the Rust programming language, which was chosen due to its performance and ease of parallelization. The main purpose of the MC code is to provide artificial data with exactly known physics and parameters, which can be used to test the ability of the TDCR model to reconstruct the input activity.

The code assumes that for each decay there are two types of scintillation light that could be emitted from the cocktail: prompt and delayed fluorescence. The photons of the prompt fluorescence are assumed to follow an exponential distribution with decay time τ_p:

$$P_p(t) = \tau_p e^{-\tau_p t}, \tag{5}$$

where $P_p(t)$ is the probability to observe a prompt photon at time t.

In practice the delayed fluorescence intensity has a complex dependence on time as it is controlled by the diffusion of triplet states. Thus, an approximate equation for the time dependence of delayed fluorescence was used in the code. The equation derived in [18] is:

$$P_d(t) = \frac{\tau_d}{4(1+\tau_d t)^{\frac{3}{2}}}, \tag{6}$$

where $P_d(t)$ is the probability to observe a delayed fluorescence photon at time t and τ_d is the delayed fluorescence decay time. Note that, with this equation the probability for delayed fluorescence does not go to zero at $t = 0$ as expected. Delayed fluorescence is produced by interaction of two triplet states yielding a singlet emission and should have some non-negligible rise time [19]. Thus, the used simplified equation could lead to increased probabilities for delayed events in the first nanoseconds after a decay. A more complete description of the delayed fluorescence intensity with time is also given in [18], but, due to the large number of unknown parameters, it was not used in this study.

In order to calculate the number of detected photons from the energy deposited in the cocktail, the MC code uses the free parameter model described in [2, 20]. The scintillator non-linearity is accounted for using Birks' ionization quenching formula [7]:

$$Q(E) = \frac{1}{E}\int_0^E \frac{dE}{1 + kB(dE/dx)}, \tag{7}$$

where dE/dx is the electron stopping power for the given cocktail parameters and kB is the Birks parameter. The semi-empirical ionization quenching formula describes the prompt fluorescence intensity as a function

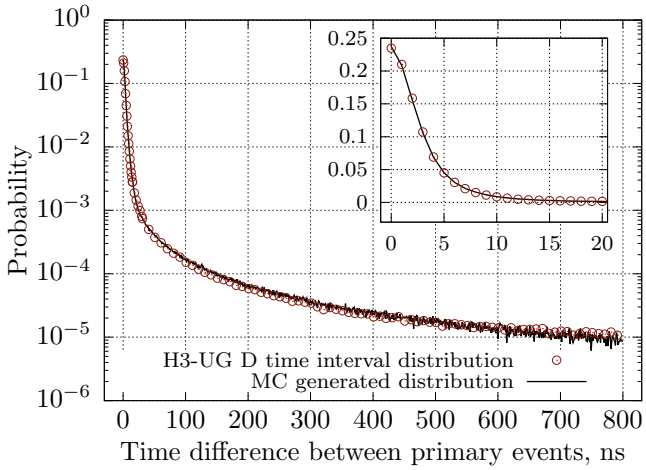

Figure 2: An example of the D time distribution of the H3-UG source and the MC generated distribution. The insert shows the same distributions in linear scale from 0 to 20 ns.

of the deposited in the scintillator energy. Note that, the intensity of delayed fluorescence has been reported to have less or even no dependence on the deposited energy [7]. Thus ionization quenching was considered only for prompt fluorescence.

The MC code works as follows:

1. An energy E is sampled from the spectrum of the nuclide, as provided by the BetaShape code [21, 22].
2. The average number of prompt fluorescence photons for the sampled energy E is calculated as:

$$\bar{n}_p = EQ(E)\lambda_p, \tag{8}$$

   where λ_p is the free parameter measured in photoelectrons per keV effective energy released in the cocktail.
3. The average number of the delayed fluorescence photons for the sampled energy E is calculated as:

$$\bar{n}_d = E\lambda_d, \tag{9}$$

   where λ_d is the free parameter for the delayed fluorescence.
4. The number of delayed fluorescence photons n_d and the number of prompt fluorescence photons n_p for the current decay are sampled from Poisson distributions with averages $\bar{n}_d$ and $\bar{n}_p$, respectively.
5. The timestamps of each of the prompt and delayed photons is sampled from the appropriate distribution, equations (5MC code for the simulation of the timing of TDCR eventsequation.2.5) and (6MC code for the simulation of the timing of TDCR eventsequation.2.6) respectively. The PMT that was hit is sampled from a weighted uniform distribution, where the weights are the relative PMT efficiencies.
6. The detected photons are sorted according to their timestamp and the primary event in each PMT is identified.
7. A value is sampled from Gaussian distribution with standard deviation σ for each of the three channels and is added to the timestamps of the primary events. The purpose of this step is to model the time jitter introduced by the detection system in the timing of the events.
8. The timestamps of the primary events are recorded in list-mode files (one for each PMT channel), similar to the comma-separated values files produced by the CAEN digitizer, i.e. one entry per line containing the timestamp of the event in picoseconds after the start.
9. The time to the next decay is sampled from an exponential distribution with the decay time of the simulated nuclide as a parameter.
10. The loop returns to step 1. and the steps are repeated until the number of requested decays is reached.

Parameter	Value
λ_p	0.57 ph.e$^-$/keV
λ_d	0.08 ph.e$^-$/keV
τ_p	0.28 s^{-1}
τ_d	0.09 s^{-1}
σ	1.25 ns
kB	100 µm/MeV

Table 2: Optimal parameters obtained from the MC code for the H3-UG source. The free parameters λ_d and λ_p are given in number of photoelectrons per keV effective energy released in the cocktail (ph.e$^-$/keV).

The list-mode files produced by the MC code can be analyzed by the same `TDCR_analysis` software as the real measurement data, thus eliminating any possible differences in data analysis.

To illustrate the performance of the MC code, the parameters of the program were varied in order to produce a good fit of the experimental time interval distribution in the D channel of the H3-UG source. The optimal parameters that were obtained are shown in Table 2Optimal parameters obtained from the MC code for the H3-UG source. The free parameters λ_d and λ_p are given in number of photoelectrons per keV effective energy released in the cocktail (ph.e$^-$/keV)table.2.

The free parameter obtained with the TDCR method for the same measurement is $\lambda = 0.68$ ph.e$^-$/keV. The obtained ratio between the delayed and total (prompt + delayed) fluorescence is 0.12. The similar ratio 0.14 was reported for DIN+PPO(1.5 g/l) cocktail in [5]. The experimental and simulated time interval distributions are shown in Figure 2An example of the D time distribution of the H3-UG source and the MC generated distribution. The insert shows the same distributions in linear scale from 0 to 20 nsfigure.2. A good agreement between the two is observed, despite the approximate equation used for the time dependence of the delayed fluorescence.

3. Results

Dependence of the counting rate on the resolving time. The `TDCR_analysis` software was used to obtain the time distributions of the studied sources and blank samples in all coincidence channels.

The relative counting rate R is calculated as:

$$R = \frac{n_i^{\text{true}}(\tau)}{n_i^{\text{true}}(2\mu\text{s})} - 100\%. \tag{10}$$

The relative counting rates in the D channels for the H3-Tol, H3-UG and H3-LLT sources as a function of the coincidence resolving time are shown in Figure 3Relative counting rate, compared to the counting rate at 2000 ns coincidence resolving time. The grey box shows the region that is enlarged in the inlet graphfigure.3. The T channel of the H3-LLT measurement is also shown to illustrate the higher loss of triple coincidences compared to double ones. For the source in the UG cocktail, the coincidence resolving time necessary to reach less than 0.1% relative counting rate in both the D and T channels is 700 ns. For the H3-LLT, the necessary time is 700 ns for the D channel and 1000 ns for the T channel. No significant change in the counting rate can be observed in all time distributions after 1200 ns, except for the T channel of the H3-LLT source. For coincidence resolving times less than 700 ns a significant loss in the D and T counting rates can be observed. The loss increases with decreasing coincidence resolving time and at 40 ns the T counting rate of the H3-LLT source is 15.4% of the counting rate at 2 µs resolving time. The losses are smaller for the H3-UG source, but nevertheless, at 40 ns the loss in the T counting rate is 6.7%. The D distribution of the H3-Tol source shows that for this cocktail most of the coincidences are recorded in the first few tens of nanoseconds, similarly to the UG, but it has more pronounced tails than the two other studied cocktails.

Similar results can be observed for the measured ^{55}Fe sources (Figure 4Relative counting rate in the D and T channels as a function of the coincidence resolving time for the Fe55-UG and Fe55-HF sourcesfigure.4).

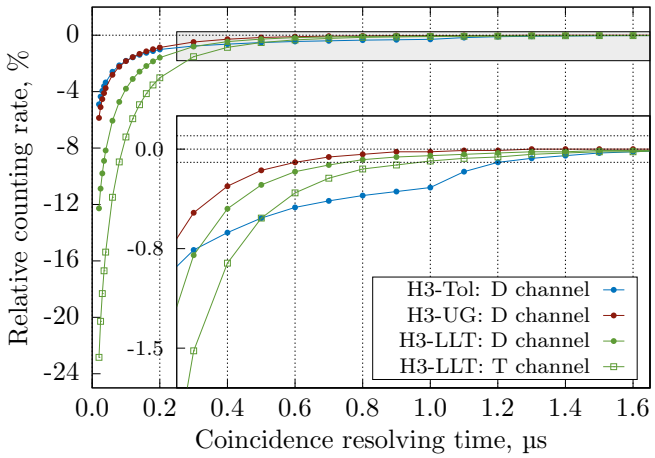

Figure 3: Relative counting rate, compared to the counting rate at 2000 ns coincidence resolving time. The grey box shows the region that is enlarged in the inlet graph.

For short coincidence resolving times a significant loss in the D and T counting rates can be observed, up to 12.9% and 24.7% in the D and T channels of the Fe55-UG measurement, respectively. The loss of coincidences is much lower for the ^{55}Fe in HionicFluor cocktail source. In that case, in order to register 99.9% of coincidence events, a 300 ns coincidence resolving time is needed, compared to 1.1 µs for the same nuclide in UG cocktail. The HionicFluor cocktail seems to have much less pronounced delayed fluorescence contribution when compared to UG and the loss of coincidences is around six times less for a given coincidence resolving time. It must be observed that, for Fe-55 source in HF, the relative counting rate is positive for D at short coincidence resolving times. This could seem strange but this is just due to a loss of T which are counted as D.

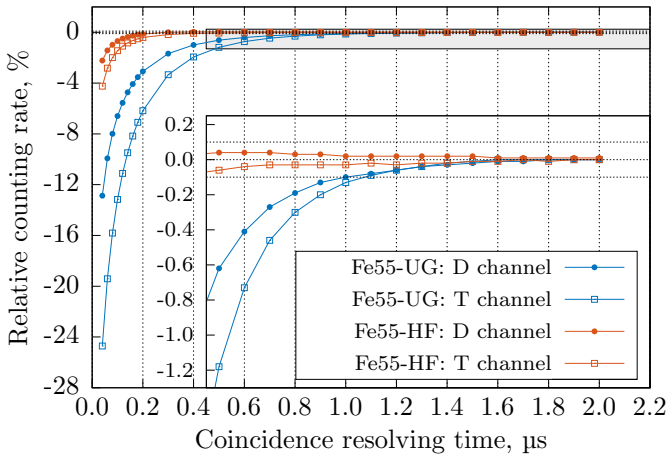

Figure 4: Relative counting rate in the D and T channels as a function of the coincidence resolving time for the Fe55-UG and Fe55-HF sources.

In the case of the higher energy nuclides ^{63}Ni and ^{14}C, the counting rate converges faster to the value at 2 µs resolving time. For the C14-UG source, a coincidence window of 100 ns is necessary to include 99.9% of D and T events and for the Ni63-UG source the necessary time is 600 ns. Despite the higher detection efficiency for these sources, there is still significant contribution of delayed photons to the total counts. The dependence on the relative counting rate on the coincidence resolving time for these sources is presented in Figure 5Relative counting rate of the D and T channels for the C14-UG and Ni63-UG sources. The dashed

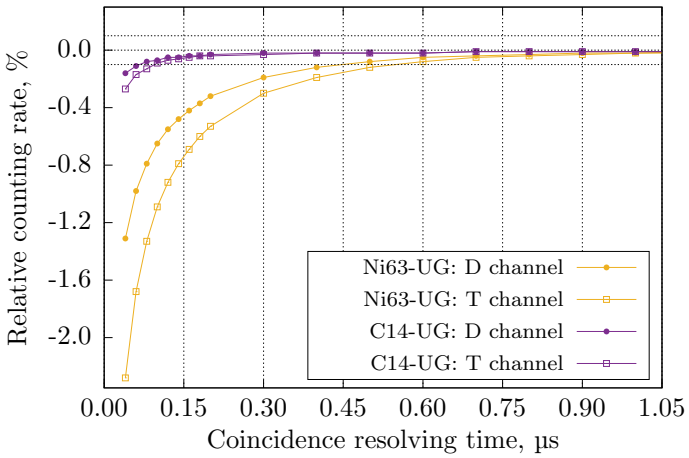

Figure 5: Relative counting rate of the D and T channels for the C14-UG and Ni63-UG sources. The dashed horizontal lines indicate relative counting rates -0.1%, 0.0% and 0.1% respectively.

horizontal lines indicate relative counting rates -0.1%, 0.0% and 0.1% respectivelyfigure.5.

Note that, for all measurements, no optical filter was used and this is the maximum detection efficiency that is achievable for the used detector with these LS-sources. If optical filters are used for the efficiency variation method used to determine the optimal kB value in the TDCR model, the decreased efficiency could lead to larger spread of the time distribution and to an increase of the fraction of the delayed fluorescence.

As prompt fluorescence has a rise time in the order of a nanosecond and decay time of a few nanoseconds for the used cocktails, it can be assumed that events registered after 15–20 ns should come from other processes such as diffusion of solvent singlet states before interaction with a fluor molecule or delayed fluorescence. Increasing the coincidence resolving time too much as to include delayed fluorescence could be undesirable if it is not accounted for properly by the TDCR model. However, it is not precisely known what is the level of overlap between the delayed and prompt fluorescence for short coincidence resolving times, especially considering that some singlet states could diffuse before interacting with a fluor molecule. It is thus important to also study the activity calculated by the TDCR model as a function of the coincidence resolving time in order to evaluate the influence of the delayed fluorescence.

Dependence of the calculated activity on the coincidence resolving time. The `TDCR_analysis` program was used to obtain the counting rates in all coincidence channels AB, BC, AC, D and T for the measured sources. The $T/AB, T/BC$ and T/AC ratios at different coincidence resolving times, from 40 to 2000 ns, were used to calculate the logical sum of double coincidences efficiency with the TDCR18 program, which is an updated version of TDCR07 [23]. The updates include the data for more LS cocktails and also the option to calculate the stopping power using the dataset published by Tan and Xia [24]. The relative activity of the measured sources as a function of the coincidence resolving time is shown in Figure 6Activity relative to the activity calculated at 2000 ns coincidence resolving time as a function of the coincidence resolving time. Note that, the activity at 2000 ns coincidence resolving time is taken only as a reference and should not be considered as the true activity of the sourcefigure.6. The relative activity is calculated using (10Dependence of the counting rate on the resolving timeequation.3.10).

The H3-Tol, H3-UG and H3-LLT sources show a similar behaviour at short coincidence window as the calculated activity for these two sources decreases with shortening of the coincidence resolving time down to 30 ns. A sharp increase in the calculated activity can be observed for shorter coincidence resolving times. Toluene+PPO, being a faster cocktail than the other two, results in a minimum calculated activity at 15 ns and a sharp increase for lower and higher coincidence resolving times. The high overestimation for very short coincidence resolving times can be explained by the higher loss of triple coincidences than double coincidences leading to a lower TDCR and an underestimation in the efficiency. From the D and

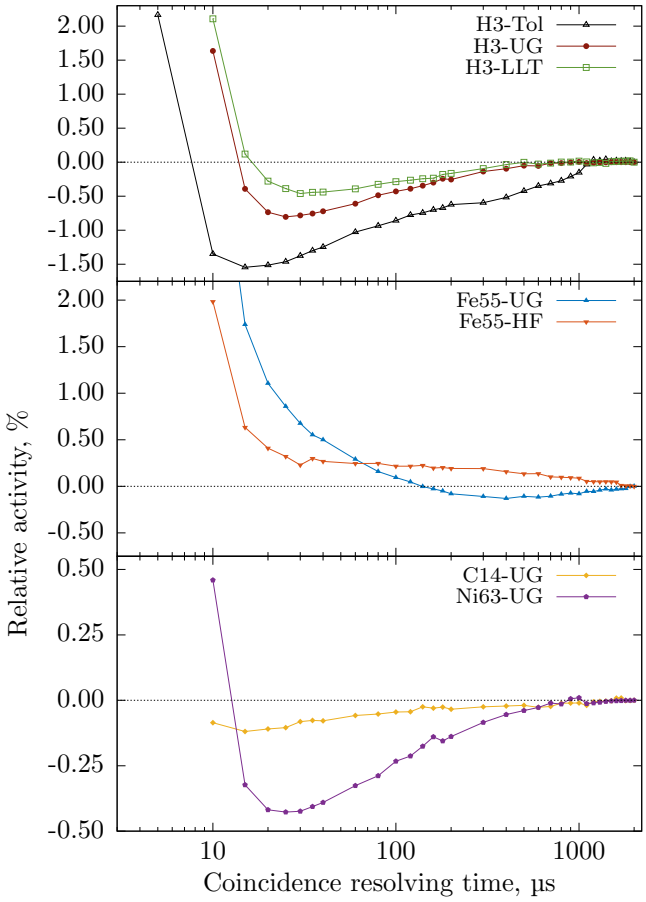

Figure 6: Activity relative to the activity calculated at 2000 ns coincidence resolving time as a function of the coincidence resolving time. Note that, the activity at 2000 ns coincidence resolving time is taken only as a reference and should not be considered as the true activity of the source.

T counting rates as a function of the coincidence resolving time for the three sources it can be seen that Toluene+PPO and UG have a significantly less pronounced delayed scintillation component compared to UG-LLT. It is intuitive to expect that the dependence of the activity on coincidence resolving time for long coincidence resolving times would be lower for cocktails exhibiting low amount of delayed fluorescence compared to cocktails where delayed fluorescence is more pronounced. The experimental results show the opposite behaviour — the calculated activity of the H3-LLT sources depends less on the coincidence resolving time than that for the H3-Tol and H3-UG sources. A possible explanation for this behaviour is given in the next subsection.

Similar relationships to the ^{3}H sources can be observed for the other two studied pure-β sources: ^{14}C and ^{63}Ni. For all studied coincidence resolving times the bias in the calculated activity of the C14-UG source is less than 0.1%. The calculated activity behaviour of the Ni63-UG source is very similar to the ^{3}H source in the same cocktail, but with a lesser dependence on the coincidence resolving time.

The electron-capture ^{55}Fe source shows a very different behaviour with the change in coincidence resolving time. For the Fe55-HF source the bias from the reference activity is positive for all coincidence resolving times. The calculated activity as a function of coincidence resolving time for the Fe55-UG source has a minimum at around 400 ns, but the increase for longer coincidence resolving times is significantly lower in comparison to the ^{3}H sources.

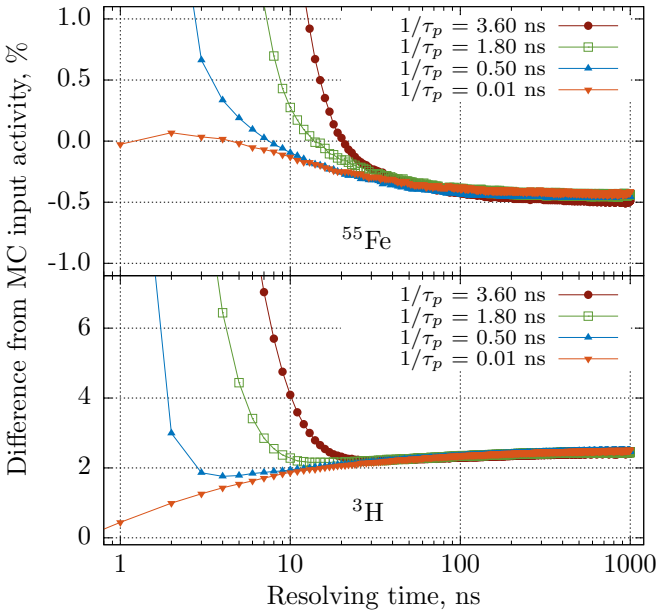

Figure 7: Dependence of the calculated activity on the coincidence resolving time for MC simulated measurements of ^{3}H and ^{55}Fe for various prompt scintillation component decay times.

Studies of the activity as a function of the coincidence resolving time using the MC code. A great advantage of the developed MC code, in comparison with the real measurements is the possibility to use the TDCR method on data from a source with precisely known activity. The main goal of the performed studies was to analyze the possible influence of scintillation light which is not affected by the ionization quenching on the calculated by the TDCR method activity. To do so, the parameters of the MC code were set to the optimal parameters determined for the H3-UG source, shown in Table 1Composition of the studied sources. The vial type of PE refers to Polyethylene vials and G + DT to borosilicate glass vial wrapped with a layer of diffusive tape. The given detection efficiency ε_D is for the logical sum of double coincidences. The final column contains the approximate mass of the aqueous solution ($m_{\mathrm{H_2O}}$) and the total mass of the scintillation cocktail (m_{tot})table.1. The gaussian jitter standard deviation σ was set to zero to facilitate the interpretation of the results. The code was used to generate list-mode files for ^{55}Fe and ^{3}H with different prompt scintillation component decay times, keeping all other parameters unchanged. In one of the runs, the decay time was set to 10 ps in order to collect all the prompt scintillation events within the first nanosecond of coincidence resolving time and observe only the delayed fluorescence influence with time. The files were processed with the `TDCR_analysis` software and the activity was calculated using the TDCR18 code from the obtained D and T counting rates as a function of the coincidence resolving time. The results from the experiment are presented in Figure 7Dependence of the calculated activity on the coincidence resolving time for MC simulated measurements of ^{3}H and ^{55}Fe for various prompt scintillation component decay timesfigure.7. Please note that in the MC code the prompt and delayed fluorescence time distributions overlap i.e. there is no coincidence resolving time that would include only prompt events and no delayed events. That is due to the approximate equation used to describe the delayed fluorescence decay time. Nevertheless, other studies [19, 25] report that an overlap between the two is to be expected.

For ^{55}Fe the calculated activity as a function of the coincidence resolving time shows a consistent downward trend which intersects the MC input activity when a certain coincidence resolving time is used, depending on the prompt decay time. If we consider the simulation with 10 ps prompt decay time, the correct activity can be calculated if the used coincidence resolving time is very short and does not include significant amount of delayed events. Increasing the coincidence resolving time leads to an underestimation of the activity, due to the detection of more delayed fluorescence photons. A significant overestimation of the

calculated activity can be observed when there is a loss of prompt events. This can be explained as for too short resolving times there is a larger loss of triple coincidences compared to double coincidences, which leads to a lower TDCR and lower estimate for the detection efficiency, thus overestimating the activity.

The same phenomenon can be observed for the ^{3}H simulation. If the resolving time is too short and there is a loss of prompt events, the activity is significantly overestimated (T losses are higher than D losses). The difference, when compared to ^{55}Fe, is that the inclusion of delayed events, not affected by ionization quenching, leads to the overestimation of the calculated activity. For the ^{3}H simulations with prompt decay time 0.5 ns and above, the activity as a function of coincidence resolving time shows a minimum value with and upward trend for longer or shorter coincidence resolving times. Only in the case of the 10 ps prompt decay time simulation with 1 ns coincidence resolving time does the calculated ^{3}H activity reach the MC reference value. For all other prompt decay times the calculated activity is overestimated by two or more percent.

The activity as a function of coincidence resolving time curves that were obtained from the MC simulations closely resemble the results obtained from the digitizer measurements (shown in Figure 6Activity relative to the activity calculated at 2000 ns coincidence resolving time as a function of the coincidence resolving time. Note that, the activity at 2000 ns coincidence resolving time is taken only as a reference and should not be considered as the true activity of the sourcefigure.6). We would like to stress here that, according to our understanding, the three effects that lead to a bias in the calculated activity are:

- unequal losses of double and triple coincidences for too short resolving times
- influence of the delayed scintillation component, which has different ionization quenching properties
- difference in the free parameter (mean number of photoelectrons per keV absorbed in the scintillator) for the prompt and the delayed scintillation

The first effect causes overestimation of the activity in all cases, as short coincidence resolving times lead to the loss of more triple coincidences than double, thus decreasing the TDCR value and underestimating the detection efficiency. The second and third effects lead to underestimation of the activity when the simulated source is monoenergetic and to overestimation in the case of ^{3}H.

The third effect is due to the fact that the classical TDCR model only considers a global free parameter value, but, as the emission mechanism is different for the prompt and the delayed fluorescence, it seems reasonable to admit that these two processes are dominated by different intrinsic light yields. In the case of ^{55}Fe, in which the detected events are mostly due to the K-shell rearrangement, the emission is quasi-monoenergetic and thus the value of the kB factor is of minor importance. Then, the observed dependence of the calculated activity versus the coincidence resolving time cannot be explained by a difference of ionization quenching between the prompt and delayed emission, but more probably by a difference in the intrinsic light yield of each scintillation component.

From these simulations it seems that for a monoenergetic source there exists a coincidence resolving time that would result in the correct activity calculation, however it will depend on the prompt and delayed fluorescence decay time and their relative contribution. The MC simulation indicates that for ^{3}H all bias effects lead to an overestimation and no coincidence resolving time can be used, that would result in the correct calculation for the activity. Moreover, the shorter the decay time of the prompt fluorescence is, the larger the difference between the minimum activity and the activity at very long coincidence resolving times would seem. This is the case seen in the measurements of Toluene+PPO and UG LLT cocktails (see Figure 6Activity relative to the activity calculated at 2000 ns coincidence resolving time as a function of the coincidence resolving time. Note that, the activity at 2000 ns coincidence resolving time is taken only as a reference and should not be considered as the true activity of the sourcefigure.6). Toluene+PPO seems to have faster prompt fluorescence than LLT, thus all of the prompt fluorescence light is gathered at shorter coincidence resolving times, when the delayed fluorescence contribution is less pronounced.

Dependence of the optimal kB parameter on the coincidence resolving time. The H3-UG, H3-LLT and Ni63-UG sources were measured also with optical filters using the same experimental setup in order to perform

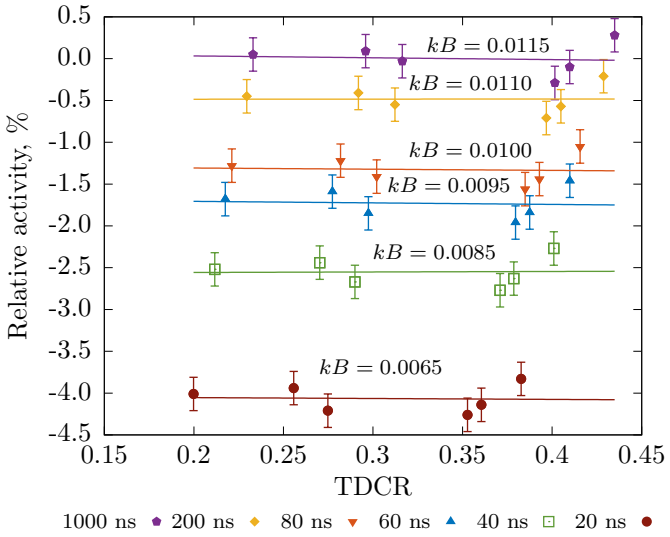

Figure 8: Relative activity of the H3-LLT as a function of the TDCR value at the optimal kB value for different coincidence resolving times. The kB value is given in units µm/MeV.

the efficiency variation method and determine the optimal kB parameter. For each measurement of a source and filter a corresponding measurement of a blank sample and filter was also performed. The list-mode files were processed with the `TDCR_analysis` program in order to obtain the counting rates in the coincidence channels as a function of the coincidence resolving time. All measurements, including blank measurements were corrected for accidental coincidences.

The counting rates at coincidence resolving times 20, 40, 60, 80, 200 and 1000 ns were used to calculate the activity of the samples for kB values from 70 µm/MeV to 160 µm/MeV with a 5 µm/MeV step. The kB value that was chosen for an optimal is the kB for which the slope of the linear fit of the activity as a function of the TDCR is closest to zero.

The optimal kB parameter for the H3-UG and Ni63-UG sources was found out to be 100 µm/MeV for all studied coincidence resolving times. For the H3-LLT source, however, a dependence of the optimal kB value with respect to the used coincidence resolving time used was observed. The calculated activity, relative to the average of the values for 1000 ns coincidence resolving time, as a function of the TDCR value for the studied coincidence resolving times is shown in Figure 8Relative activity of the H3-LLT as a function of the TDCR value at the optimal kB value for different coincidence resolving times. The kB value is given in units µm/MeVfigure.8. The kB value that results in the smallest slope for 40 ns coincidence resolving time is at 85 µm/MeV and for 1000 ns it is 115 µm/MeV.

Another source (H3-LLT2) from the same LLT cocktail and tritiated water solution with similar activity was prepared and measured on the RCTD1 [17] detector at LNHB. The PMTs of the TDCR counter were directly connected to the nanoTDCR [10], a device dedicated to TDCR measurements. The nanoTDCR is capable of simultaneous measurements with two different coincidence windows, thus it is a suitable device to test the effect of the used resolving time on the kB parameter, determined by the efficiency variation method. The H3-LLT2 source and its blank sample were measured with a series of optical grey filters. All measurements were performed simultaneously with coincidence resolving times 40 ns and 200 ns and 10 µs dead-time base duration using the common dead-time logic. The results of the experiment are shown in Figure 9Relative activity of the H3-LLT2 as a function of the TDCR value at the optimal kB value for coincidence resolving times 40 ns and 200 ns. The linear fit with the smallest slope is shown with a solid line. The values on the right are the kB parameter given in units µm/MeV. The two plots have the same scale and range on the abscissa. The measurements were carried out on the RCTD1 system and nanoTDCR device and the efficiency was varied by means of gray filtersfigure.9. The measurements of the H3-LLT2 source confirm the observed behaviour of the H3-LLT source. The kB value that gives the smallest slope (fit shown

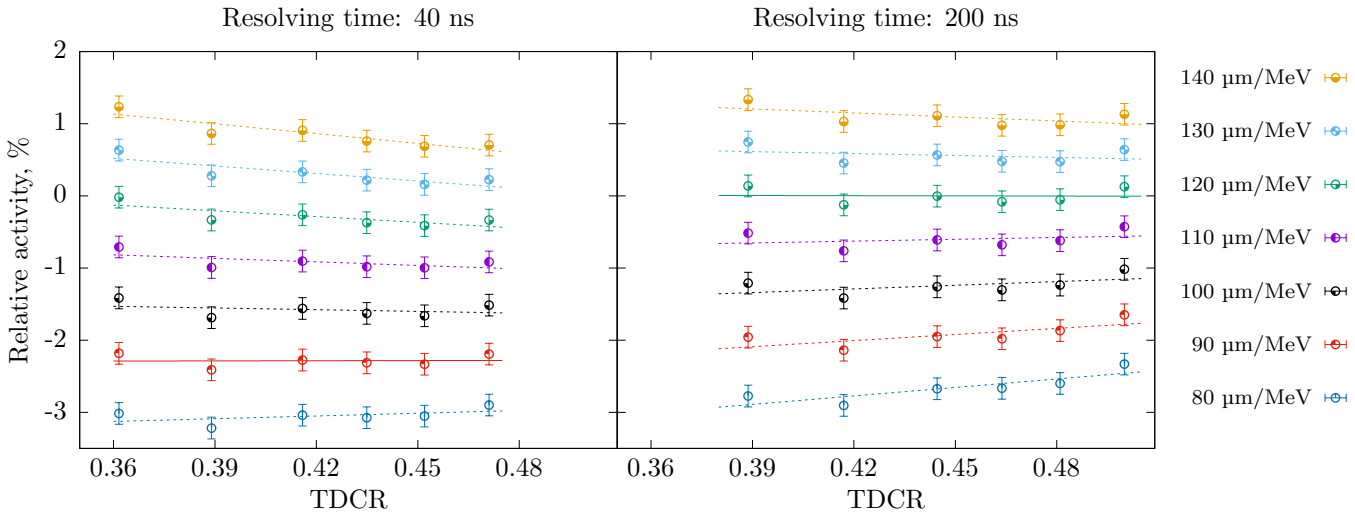

Figure 9: Relative activity of the H3-LLT2 as a function of the TDCR value at the optimal kB value for coincidence resolving times 40 ns and 200 ns. The linear fit with the smallest slope is shown with a solid line. The values on the right are the kB parameter given in units µm/MeV. The two plots have the same scale and range on the abscissa. The measurements were carried out on the RCTD1 system and nanoTDCR device and the efficiency was varied by means of gray filters.

with solid line) for 40 ns coincidence resolving time is 90 µm/MeV and for 200 ns it is 120 µm/MeV. The wider coincidence resolving time also leads to a significant increase in the TDCR values of all measurements.

When considering the counting rates as a function of the coincidence resolving time for the studied sources, it would seem that for LLT the delayed fluorescence is more pronounced compared to UG. This could explain why increasing the coincidence resolving time and including more delayed fluorescence photons leads to some dependence of the optimal kB parameter. As it is the only adjustable parameter of the TDCR model, it is possible that it compensates for some dependence of the calculated activity on the detection efficiency caused by delayed fluorescence, which is not included in the model.

It is important to note the large difference between the optimal kB parameters obtained for H3-LLT for 20 ns and 40 ns coincidence resolving time (see Figure 8Relative activity of the H3-LLT as a function of the TDCR value at the optimal kB value for different coincidence resolving times. The kB value is given in units µm/MeVfigure.8). In that range we would expect to select a resolving time which is long enough to include all prompt events and short enough to minimize the delayed fluorescence contribution. The strong dependence of the observed kB parameter and thus calculated activity in this range would prevent the determination of such a coincidence resolving time. These results suggest that UG LLT is unsuitable for standardization of ^{3}H with the TDCR method, due to its large delayed fluorescence contribution.

Comparison of efficiency variation with gray filters and chemical quenching. There are two types of efficiency variation techniques commonly used in TDCR measurements: placing optical gray filters between the LS sample and detector and chemical quenching. Both methods differ in the way the scintillation light is reduced. The gray filter absorbs part of the light emitted by the LS cocktail and thus affects both prompt and delayed fluorescence in the same way. The chemical quenching is achieved by introducing chemical scavengers of excited solvent molecules, which leads to a decrease in the light emission yield [15]. A third technique for efficiency variation by means of PMT defocusing also exists, but it was not used in this study.

In order to study the influence of the delayed fluorescence on the calculated activity with different efficiency variation methods the set of seven ^{3}H in UG LS-sources with added nitromethane H3-UGQ were used (see Table 1Composition of the studied sources. The vial type of PE refers to Polyethylene vials and G + DT to borosilicate glass vial wrapped with a layer of diffusive tape. The given detection efficiency ε_D is for the logical sum of double coincidences. The final column contains the approximate mass of the aqueous solution ($m_{\mathrm{H_2O}}$) and the total mass of the scintillation cocktail (m_{tot})table.1). The unquenched source was

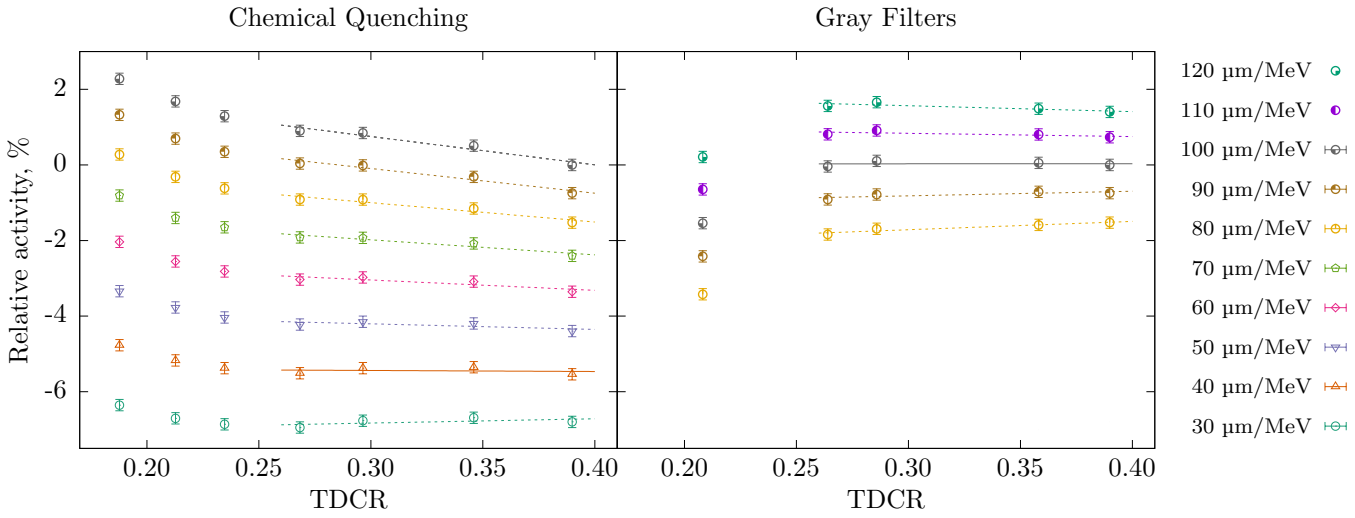

Figure 10: Relative activity of the H3-UG as a function of the TDCR value. The linear fit with the smallest slope is shown with a solid line. The values on the right are the kB parameter given in units µm/MeV. The two plots have the same scale and range on the abscissa. The measurements were performed using the miniTDCR system and the CAEN digitizer.

also measured with a set of gray filters. All measurements were performed using the miniTDCR with the CAEN DT5751 digitizer and `TDCR_analysis` software. The coincidence resolving time used in all cases is 40 ns.

The results of the experiment are shown in Figure 10Relative activity of the H3-UG as a function of the TDCR value. The linear fit with the smallest slope is shown with a solid line. The values on the right are the kB parameter given in units µm/MeV. The two plots have the same scale and range on the abscissa. The measurements were performed using the miniTDCR system and the CAEN digitizerfigure.10. In the left and right plots, the highest efficiency data points are from the same measurements of the unquenched sample. The calculated activities of the six nitromethane quenched LS-sources and the unquenched sample are shown on the left for different values of the kB parameter from 30 to 100 µm/MeV. The calculated activities of the unquenched sample with different gray filters is shown on the right for kB values from 80 to 120 µm/MeV.

The optimal kB value was found out to be 40 µm/MeV for efficiency variation with chemical quenching and 100 µm/MeV with gray filters. Moreover, it is interesting to note that for TDCR values lower than 0.25 there is an upward trend for the activity as a function of efficiency when using chemical filters. This is contrary to the downward trend observed for gray filters in the same range of TDCR values.

One possible explanation for the different behaviour of chemical quenching and gray filters is that the added nitromethane does not quench delayed fluorescence in the same manner as prompt fluorescence. A comparison of the time interval distributions after applying gray filters or chemical quenching is shown in Figure 11Time interval distributions in the D channel of the H3-UGQ set of sources. The H3-UGQ1 LS-source is unquenched, UGQ3 and UGQ7 are quenched with nitromethane and F86% and F64% are the unquenched source with gray filtersfigure.11. The solid black line is the D time interval distribution of the unquenched H3-UGQ1 source. The dashed lines are the distributions of the chemically quenched samples and the dash/dot lines are the distributions of the unquenched sample with gray filters.

From the time interval distributions it can be seen that the chemical quenching with nitromethane does not affect significantly the delayed fluorescence and the probability for events after 20 ns is higher compared to the unquenched sample. In the first 10 ns the distributions of the chemically quenched samples closely resemble the distribution of the unquenched LS-source. The D distribution is significantly changed in the same time interval if gray filters are used. The ratio of prompt to delayed photons emitted remains constant when using optical filters as both types of fluorescence have the same wavelength. Nevertheless, when the

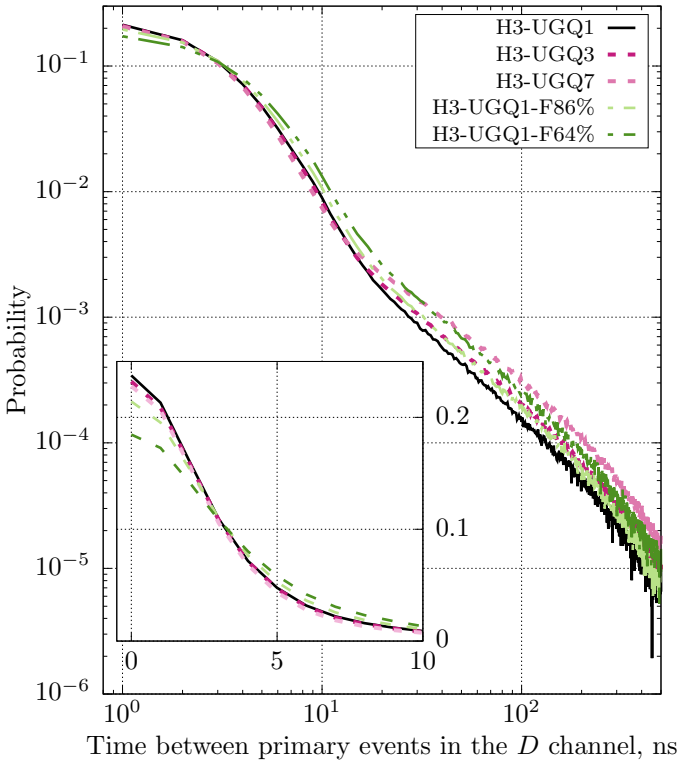

Figure 11: Time interval distributions in the D channel of the H3-UGQ set of sources. The H3-UGQ1 LS-source is unquenched, UGQ3 and UGQ7 are quenched with nitromethane and F86% and F64% are the unquenched source with gray filters.

total number of photons is reduced, the probability for a delayed photon to be a primary event increases. For example, if the average number of photons is high, then the first incoming events in each PMT would be prompt events as delayed events are slower on average. On the other hand, if the average number of prompt photons is close to 1, then some delayed photons should be detected in order to have a double or triple coincidence. Another effect of gray filters on the time distribution is that when reducing the number of detected photons, the average time interval between two photons increases, thus the significant decrease of the probability for time intervals in the order of few nanoseconds. The latter effect should be present also in the time interval distributions with chemical quenching. The fact that the distribution is not significantly changed in the first few nanoseconds suggests that nitromethane quenches some component of the scintillation light other than that responsible for very prompt events.

From the theory of the scintillation process in organic materials there are two processes that lead to energy transfer between the solvent and fluor molecules: non-radiative transfer to the fluor from an excited solvent molecule (Förster process) and diffusion controlled non-radiative transfer [7]. The non-radiative transfer between solvent and solute can be interrupted if the excited solvent molecule interacts with a molecule of the quencher before reaching the fluor. Thus, solvent molecules that are excited in the immediate vicinity of a fluor molecule would produce scintillation light promptly. If, however, solvent molecules need to undergo diffusion before interacting with a fluor molecule, then the probability for interaction with a quencher molecule increases with time. Such process could possibly explain the reduced probability for events between 5 and 15 ns with nitromethane compared to gray filters.

The selective quenching of the prompt fluorescence by nitromethane would lead to increased overestimation of activity for higher concentrations. This introduces a dependence of the calculated activity from the detection efficiency which is compensated by a lower kB parameter. Further studies are needed to quantify the magnitude of the possible underestimation of the kB value when applying the efficiency variation method with chemical quenching.

4. Discussion

4.1. A note on the energy transfer in a binary liquid scintillator, formation of excited states and the emission of prompt and deayed fluorescence

A typical liquid scintillation cocktail with a wavelength shifter is composed of an aromatic solvent (i.e. toluene, pseudocumene, DIN...) in which a primary fluorescent molecule (e.g. PPO) is dissolved at a concentration of about 5 to 7 g/L and a wavelength shifter is present at a concentration of about 0.5 g/L. As the energy transfer between the solvent and the primary fluorescent molecule is non-radiative and the energy transfer between the primary and secondary fluorescent molecules is radiative, the presence of the wavelength shifter does not interfere in the following considerations concerning non-radiative energy transfer. The real scintillators also include surfactant molecules to stabilize water micelles in the organic phase, but these molecules are also based on aromatic compounds and can be considered as part of the solvent.

The interaction of electrons with the liquid scintillator mainly concerns the solvent, as this is the dominant specie. The electrons lose their energy by collision creating ionized and excited molecules localized around the track of the particle. The fast electrons (i.e. over a few tens of keV) create excited zones with a characteristic size, for which the Coulomb attraction is lower than kT, which in practice corresponds to a few tens of nm. When the energy of the electron decreases, the linear energy transfer, dE/dx, increases and the excited and ionized molecules are concentrated in small blobs, spurs and short tracks localized around the initial electron track. The main primary energy transfer processes are: 1. excitation into π-electrons singlet states (S_N), 2. π-electrons ionization and 3. excitation and ionization of electrons other than π-electrons [7]. The latter processes lead to dissipation of energy as heat. The S_N states directly created by excitation quickly decay into S_1 states by non-radiative transitions. The ionized molecules quickly recombine (within 10^{-11} s) to form excited molecules in highly excited singlets and triplet states (S_N and T_N). The direct formation of excited states T_1 and S_1 have low probability, due respectively to spin and symmetry selection rules. After ion-recombination, the initial probability of creation of S_N and T_N states is statistically similar, but as there are three possible T_N states, there are three times more T_N excited molecules than S_N molecules. Then the highly excited states de-excite towards the primary excited levels S_1 and T_1, in a typical time scale of 10^{-11} to 10^{-10} s. The ratio of S_1 to T_1 states depends on the nature of the solvent and on the linear energy transfer (LET) of the ionizing radiation. The ionization processes are more probable for high LET, thus for low-energy electrons. Voltz [26] mentioned that this ratio is about 3.3 for γ-rays (in fact from the electrons created by the interaction of a γ-ray with the scintillator).

After the formation of the S_1 and T_1 states, at a time scale of a few ns, the main energy transfer phenomena can be summarized by the following equations, mentioned by Voltz and Laustriat [27], but neglecting the reactions with low probability.

1. $S_1 \rightarrow S_0$ or $S_1 + S_0 \rightarrow S_0 + S_0$ — de-excitation of singlets
2. $S_1 + S_0 \rightarrow S_0 + S_1$ — energy migration in the solvent (can also involve excimer formation and dissociation [28])
3. $S_1 + \mathrm{Q} \rightarrow S_0 + \mathrm{Q}$ — chemical quenching of singlets
4. $T_1 \rightarrow S_0$ — de-excitation of triplets
5. $T_1 + \mathrm{Q} \rightarrow S_0 + \mathrm{Q}$ — chemical quenching of triplets
6. $T_1 + T_1 \rightarrow S_1 + S_0$ — annihilation triplet-triplet creating a singlet state
7. $T_1 + T_1 \rightarrow T_1 + S_0$ — annihilation triplet-triplet
8. $S_1 + F_0 \rightarrow F_1 + S_0$ — energy transfer to the fluorescent molecule (Förster process)
9. $F_1 \rightarrow F_0 + h\nu$ — de-excitation of the fluorescent molecule and light emission

The concentration of S_0, F_0 and Q are homogeneous in the scintillator, which is not the case for S_1 and T_1 which are localized in small volumes, at time scales of about 10^{-10} s. According to Voltz and Laustriat [27], no significant bimolecular $S_1 + S_1 \rightarrow S_0 + S_0$ happen, and they conclude that the ionization quenching phenomena, i.e. the initial recombination of excited singlet species created in a close vicinity, is not significant at this stage and thus this phenomenon concerns mainly the excited states S_3 and S_2 [28]. The main argument supporting this assertion is that the ionization quenching does not affect S_1 lifetime. It

should be noted that this is not the case for T_1 species, where the bimolecular reaction (7) is favorised by the local concentration of F_1 states, but this reaction is also in competition with (6) which causes delayed scintillation. Birks [7], noticed that: "The ionization quenching mainly affects the intensity of the fast scintillation component, and has much less effect on the intensity of the slow component" (sic). This implies that the ionization quenching is not similar for the singlets and triplets states.

The typical lifetime of S_1 states is a few ns, much shorter than the lifetime of T_1 states, typically a few hundreds of ns, depending on the nature of the solvent. The lifetime of F_1 states is lower than a ns and generally the quantum yield of equation (9) is high, the radiative de-excitation of fluorescent molecules being close to one.

This led to the following conclusions:

- The initial amount of triplet states depends on the LET of the ionizing radiation, but in all cases should not be ignored and thus delayed scintillation is to be expected.
- Singlet states give the prompt scintillation and triplet states give the delayed scintillation. Nevertheless, even if the initial number of triplet states is not negligible, the total delayed light intensity is generally lower than the prompt emission intensity, due to the necessity of bimolecular $T_1 + T_1$ reaction to create S_1 states giving the delayed emission. Birks [7], claims that the delayed scintillation represents about 10% of the prompt emission but of course this value is very dependent on the nature of the LS cocktail.
- The ionization quenching of singlet states occurs during the initial electron-solvent interaction, at the higher S_N states and at time scales lower than a nanosecond.
- The ionization quenching of triplet states also occurs during the initial electron-solvent interaction, but this phenomenon can also concern $T_1 + T_1$ annihilation at time scales greater than a nanosecond. A high value of the LET promotes the proximity of excited molecules and thus increases the probability of $T_1 + T_1$ reaction with a reduction of light emission (reaction (7)) and an increase of delayed emission (reaction (6)).
- The action of chemical quenching of S_1 and T_1 is similar (reactions (3) and (5)), but it can be supposed that the reaction constants could be different, and thus the chemically quenched proportions of prompt and delayed emission could differ. The Birks formula is a semi-empirical model relative to the prompt scintillation and the kB value, which is considered a property of the LS cocktail, could be different for the delayed emission.

4.2. On the influence of the prompt and delayed fluorescence on the TDCR measurement results

The results described in this paper show that there could be a significant dependence on the measured coincidence counting rates from the used coincidence resolving time. The necessary coincidence resolving times in order to detect 99.9% of coincidences for the studied LS-sources were found to be 700 ns for the ^{3}H in UG source, 1 µs for the ^{3}H in UG LLT source and 1.2 µs for the ^{3}H in Toluene+PPO source. Both studied ^{55}Fe sources also show a large time spread of the coincidences where for the ^{55}Fe in HionicFluor source the necessary coincidence resolving time is 300 ns and for the same nuclide in UG cocktail it is 1.1 µs. The observed losses at short coincidence resolving times for the studied ^{14}C and ^{63}Ni sources are lower than for the other nuclides. The necessary coincidence resolving time to achieve a bias lower than 0.1% is 100 ns for the ^{14}C in UG source and 600 ns for ^{63}Ni in UG source.

The TDCR model for the calculation of detection efficiency seems to compensate well for the large loss of coincidences at short coincidence resolving times, nevertheless, a significant dependence of the calculated activity on the coincidence resolving time was observed for ^{3}H, ^{55}Fe and ^{63}Ni. A large overestimation of the calculated activity can be observed for these nuclides at coincidence resolving times shorter than 20 ns. For the pure-β sources, the relationship has a minimum between 15 ns and 30 ns.

A MC code was used to simulate TDCR measurements of ^{3}H and ^{55}Fe with assumptions of exponentially decaying prompt fluorescence and delayed fluorescence that does not experience ionization quenching. The

calculated activity as a function of the coincidence resolving time of the simulated data closely resembles the true measurements. For short coincidence resolving times the activity is overestimated for both studied nuclides due to the larger loss of triple coincidences compared to double coincidences which leads to a decreased TDCR and underestimation of the detection efficiency. When including delayed fluorescence, however, the calculated activity is underestimated in the case of ^{55}Fe and overestimated in the case of ^{3}H. This suggests that if delayed fluorescence is present in the cocktail, no coincidence resolving time exists that results in the correct activity calculation with the TDCR model, as both bias effects lead to an overestimation. For the simulated ^{55}Fe measurements a coincidence resolving time can be found for which the calculated activity is equal to the true activity, however, it depends on the prompt fluorescence decay time and the delayed fluorescence contribution.

The MC studies indicate that, for ^{3}H and nuclides with a similar spectrum, the minimum calculated activity would be closest to the real one. Increasing the coincidence resolving time beyond that which results in the minimum calculated activity, would only introduce more delayed fluorescence photons and increase the overestimation of the activity. However, if the delayed fluorescence is not negligible in comparison with the prompt, then it is possible that even the minimum activity is still significantly overestimated. Thus, it would seem that the use of LS cocktails that exhibit lower delayed fluorescence contribution is preferable.

The efficiency variation method for obtaining the optimal kB parameter used in the TDCR model was applied to two of the ^{3}H sources and the ^{63}Ni source. No dependence of the optimal kB value on the used coincidence resolving time was observed for the ^{3}H in UG and the ^{63}Ni sources. A significant dependence was observed for the ^{3}H in UG LLT source; the kB value that leads to the smallest dependence on the calculated activity from the TDCR value is 85 µm/MeV for 40 ns coincidence resolving time and 115 µm/MeV for 1 µs coincidence resolving time. A similar source, ^{3}H in UG LLT, was measured on a different TDCR counter with the nanoTDCR device using its feature for simultaneous measurements with coincidence resolving times 40 ns and 200 ns. The optimal kB parameter for the shorter coincidence resolving time was found out to be 90 µm/MeV and for the longer one: 120 µm/MeV. These experiments imply that if the delayed fluorescence contribution is significant, as is the case for ^{3}H in UG LLT, then efficiency variation could be an unreliable method to determine the optimal kB parameter.

A set of ^{3}H in UG LS-sources chemically quenched with different amounts of nitromethane were measured to determine the optimal kB parameter. An unquenched source from the set was measured also with a set of gray filters in order to compare the kB parameters obtained by the two approaches. The kB parameter obtained from chemical quenching is 40 µm/MeV and from gray filters is 100 µm/MeV. A possible explanation for this discrepancy is that nitromethane quenches singlet states more so than triplet states, thus increasing the relative contribution of the delayed fluorescence leading to a higher overestimation of activity. This introduces a dependence of the calculated activity on the efficiency which is compensated by the kB parameter, being the only adjustable parameter in the TDCR model.

When it was observed that, for low-energy radionuclides, some real coincidences are lost when a coincidence resolving time of 40 ns is used, it made sense to admit that the coincidence resolving time must be extended to record the maximum number of events. In fact, this is only a reasonable approach if the physics describing the prompt and delayed emission is modelled in the TDCR calculation. A closer look at this physics reveals that the ionization quenching phenomenon described by the Birks law only concerns the prompt light emission. Moreover, due to the difference in the light emission process, the intrinsic light yield of the scintillator and thus the figure of merit used to calculate the detection efficiency is likely to be different for the two components. This is also the case for the effects of the chemical quenching, which generally occurs in LS sources because of the presence of oxygen.

From these considerations, three approaches could be used: the first one would be to use short coincidence resolving time, in order to avoid a big influence of the delayed light emission. A value of about 50 ns, close to the 40 ns used in the MAC3 module [6] seems to be a good compromise, but this value does not completely suppress the effects of the delayed fluorescence and it should be noted that it is only an approximation. The second one would be to use a newly developed or already existing LS cocktail that strongly diminishes the undesirable influence of delayed fluorescence. The third and most satisfactory approach would be to include a model of the delayed fluorescence in the TDCR calculation. This would include a term for the ionization quenching of T excited states, but also a kinetic model of triplet annihilation reactions considering the initial

spatial inhomogeneity and the molecular diffusion phenomena together with the energy transfer mechanisms between the excited molecules. Of course, this model would not be straightforward and would involve more parameters than only the kB value (e.g. kB for T states, diffusion coefficients, different figures of merit...). These parameters could not be determined from the TDCR value of a single counting experiment and more characterisations would be needed, e.g. from pulses time distributions.

Eventually, it would also be necessary to determine the standard activity of the radionuclides of interest by another method than TDCR LSC, because all the bias discussed in this paper are relative to more or less arbitrary reference values. This is not an easy task when dealing with relative uncertainties lower than one percent, and for pure beta radionuclides for which alternative primary measurement methods are seldom or even inexistent. For tritium, possible methods could be the measurement of the ingrowth of ^{3}He or internal gas counting after water to hydrogen conversion, but previous experiments [29] showed that it is difficult to reach under percent relative uncertainties with these methods. For ^{55}Fe, measurements based on X-ray or Auger emission can be used, but these measurements generally depend on the uncertainties of nuclear and atomic data, namely the capture probabilities and the fluorescence yields. A promising experiment would be the use of a 4-π cryogenic detector, in which all electron capture would give a detectable signal [30].

5. Conclusions

In this work it is shown that, despite the recent development of corrections for accidental coincidences in TDCR counting, it is not advisable to use longer coincidence resolving times in TDCR standardization of low energy β-emitters. We show that both the detected coincidences and the estimated activities depend on the coincidence resolving time. This dependence is attributed to the unequal loss of double and triple coincidences as well as to the different ionization quenching properties of the delayed scintillation component. Studies of MC generated artificial data shows that if the used cocktail has a non-negligible delayed fluorescence contribution, then, even for short coincidence resolving times, the activity of a low energy β-emitter would be overestimated.

In conclusion, using a short coincidence resolving time does not reject completely the detection of the delayed fluorescence which is not correctly modelled by the ionization quenching model. Moreover, it suppresses part of the prompt emission, as the two phenomena overlap in time. Thus, it is a compromise and the only way to use all the light emitted by the scintillator and to maximize the detection efficiency is to modify the TDCR model to include both the prompt and delayed emission.

Acknowledgements

The experiments for this work were performed during the stay of one of us (Ch. D.) at LNHB with a financial support from the French Laboratoire National de Métrologie et d'Essais (LNE). This financial support is gratefully acknowledged.

This work is supported by the Bulgarian National Scientific Research Fund under contract № KP–06–H38/9 from 06.12.19 (TDCX).

References

[1] R. Broda, P. Cassette, K. Kossert, Radionuclide metrology using liquid scintillation counting, Metrologia 44 (4) (2007) S36.

[2] R. Broda, K. Pochwalski, T. Radoszewski, Calculation of liquid-scintillation detector efficiency, International Journal of Radiation Applications and Instrumentation. Part A. Applied Radiation and Isotopes 39 (2) (1988) 159–164. doi:10.1016/0883-2889(88)90161-x.

[3] C. Bobin, J. Bouchard, B. Censier, First results in the development of an on-line digital counting platform dedicated to primary measurements, Applied Radiation and Isotopes 68 (7-8) (2010) 1519–1522. doi:10.1016/j.apradiso.2009.11.067.

[4] C. Dutsov, K. Mitev, P. Cassette, V. Jordanov, Study of two different coincidence counting algorithms in TDCR measurements, Applied Radiation and Isotopes 154 (2019) 108895. doi:10.1016/j.apradiso.2019.108895.

[5] P. Lombardi, F. Ortica, G. Ranucci, A. Romani, Decay time and pulse shape discrimination of liquid scintillators based on novel solvents, Nuclear Instruments and Methods in Physics Research Section A: Accelerators, Spectrometers, Detectors and Associated Equipment 701 (2013) 133–144. doi:10.1016/j.nima.2012.10.061.
URL https://doi.org/10.1016/j.nima.2012.10.061
[6] J. Bouchard, P. Cassette, MAC3: an electronic module for the processing of pulses delivered by a three photomultiplier liquid scintillation counting system, Applied Radiation and Isotopes 52 (3) (2000) 669–672. doi:10.1016/s0969-8043(99)00228-6.
[7] J. B. Birks, The Theory and Practice of Scintillation Counting, Pergamon Press, Oxford, 1964.
[8] L. Mo, L. J. Bignell, T. Steele, D. Alexiev, Activity measurements of ^{3}H using the TDCR method and observation of source stability, Applied Radiation and Isotopes 68 (7-8) (2010) 1540–1542. doi:10.1016/j.apradiso.2009.11.059.
URL https://doi.org/10.1016/j.apradiso.2009.11.059
[9] E. Halter, C. Thiam, C. Bobin, J. Bouchard, D. Chambellan, B. Chauvenet, M. Hamel, L. Rocha, M. Trocmé, R. Woo, First TDCR measurements at low energies using a miniature x-ray tube, Applied Radiation and Isotopes 93 (2014) 7–12. doi:10.1016/j.apradiso.2014.03.007.
URL https://doi.org/10.1016/j.apradiso.2014.03.007
[10] V. Jordanov, P. Cassette, C. Dutsov, K. Mitev, Development and applications of a miniature TDCR acquisition system for in-situ radionuclide metrology, Nuclear Instruments and Methods in Physics Research Section A: Accelerators, Spectrometers, Detectors and Associated Equipment 954 (2020) 161202. doi:10.1016/j.nima.2018.09.037.
[11] M. Capogni, P. D. Felice, A prototype of a portable TDCR system at ENEA, Applied Radiation and Isotopes 93 (2014) 45–51. doi:10.1016/j.apradiso.2014.03.021.
[12] T. Steele, L. Mo, L. Bignell, M. Smith, D. Alexiev, FASEA: A FPGA acquisition system and software event analysis for liquid scintillation counting, Nuclear Instruments and Methods in Physics Research Section A: Accelerators, Spectrometers, Detectors and Associated Equipment 609 (2-3) (2009) 217–220. doi:10.1016/j.nima.2009.07.045.
[13] K. Mitev, P. Cassette, V. Jordanov, H. R. Liu, C. Dutsov, Design and performance of a miniature TDCR counting system, Journal of Radioanalytical and Nuclear Chemistry 314 (2) (2017) 583–589. doi:10.1007/s10967-017-5451-3.
[14] C. Dutsov, P. Cassette, B. Sabot, K. Mitev, Evaluation of the accidental coincidence counting rates in TDCR counting, Nuclear Instruments and Methods in Physics Research Section A: Accelerators, Spectrometers, Detectors and Associated Equipment 977 (2020) 164292. doi:10.1016/j.nima.2020.164292.
URL https://doi.org/10.1016/j.nima.2020.164292
[15] P. Cassette, R. Broda, D. Hainos, T. Terlikowska, Analysis of detection-efficiency variation techniques for the implementation of the TDCR method in liquid scintillation counting, Applied Radiation and Isotopes 52 (3) (2000) 643–648. doi:10.1016/s0969-8043(99)00224-9.
URL https://doi.org/10.1016/s0969-8043(99)00224-9
[16] CAEN DT5751 digitizer manual, https://www.caen.it/products/dt5751/ (2020).
[17] P. Cassette, R. Vatin, Experimental evaluation of TDCR models for the 3 PM liquid scintillation counter, Nuclear Instruments and Methods in Physics Research Section A: Accelerators, Spectrometers, Detectors and Associated Equipment 312 (1-2) (1992) 95–99. doi:10.1016/0168-9002(92)90135-q.
URL https://doi.org/10.1016/0168-9002(92)90135-q
[18] T. A. King, R. Voltz, The time dependence of scintillation intensity in aromatic materials, Proceedings of the Royal Society of London. Series A. Mathematical and Physical Sciences 289 (1418) (1966) 424–439. doi:10.1098/rspa.1966.0021.
[19] G. Laustriat, The luminescence decay of organic scintillators, Molecular Crystals 4 (1-4) (1968) 127–145. doi:10.1080/15421406808082905.
URL https://doi.org/10.1080/15421406808082905
[20] A. G. Malonda, B. M. Coursey, Calculation of beta-particle counting efficiency for liquid-scintillation systems with three phototubes, International Journal of Radiation Applications and Instrumentation. Part A. Applied Radiation and Isotopes 39 (12) (1988) 1191–1196. doi:10.1016/0883-2889(88)90098-6.
URL https://doi.org/10.1016/0883-2889(88)90098-6
[21] X. Mougeot, Reliability of usual assumptions in the calculation of β and ν spectra, Physical Review C 91 (5) (May 2015). doi:10.1103/physrevc.91.055504.
URL https://doi.org/10.1103/physrevc.91.055504
[22] X. Mougeot, Erratum: Reliability of usual assumptions in the calculation of β and ν spectra [phys. rev. c91, 055504 (2015)], Physical Review C 92 (5) (Nov. 2015). doi:10.1103/physrevc.92.059902.
URL https://doi.org/10.1103/physrevc.92.059902
[23] Detection efficiency calculation for pure-beta radionuclides, program with short tutorial, http://www.nucleide.org/ICRM_LSCWG/icrmsoftware.htm.
[24] Z. Tan, Y. Xia, Stopping power and mean free path for low-energy electrons in ten scintillators over energy range of 20–20, 000ev, Applied Radiation and Isotopes 70 (1) (2012) 296–300. doi:10.1016/j.apradiso.2011.08.012.
URL https://doi.org/10.1016/j.apradiso.2011.08.012
[25] C. Fuchs, F. Heisel, R. Voltz, Formation of excited singlet states in irradiated aromatic liquids, The Journal of Physical Chemistry 76 (25) (1972) 3867–3875. doi:10.1021/j100669a033.
URL https://doi.org/10.1021/j100669a033
[26] R. Voltz, H. Dupont, G. Laustriat, Radioluminescence des milieux organiques. II. vérification expérimentale de l'étude cinétique, Journal de Physique 29 (4) (1968) 297–305. doi:10.1051/jphys:01968002904029700.
URL https://doi.org/10.1051/jphys:01968002904029700
[27] R. Voltz, G. Laustriat, Radioluminescence des milieux organiques i. étude cinétique, Journal de Physique 29 (2-3) (1968)

159–166. doi:10.1051/jphys:01968002902-3015900.
URL https://doi.org/10.1051/jphys:01968002902-3015900

[28] J. B. Birks, J. C. Conte, Excimer fluorescence. xi. solvent-solute energy transfer, Proceedings of the Royal Society of London. Series A, Mathematical and Physical Sciences 303 (1472) (1968) 85–95.
URL http://www.jstor.org/stable/2415866

[29] P. Jean-Baptiste, P. Cassette, E. Fourré, I. Tartès, A. Dapoigny, Measurement of the french national tritiated-water standard by helium-3 mass spectrometry, Applied Radiation and Isotopes 87 (2014) 157–161. doi:10.1016/j.apradiso.2013.11.126.
URL https://doi.org/10.1016/j.apradiso.2013.11.126

[30] M. Loidl, M. Rodrigues, R. Mariam, Measurement of the electron capture probabilities of ^{55}Fe with a metallic magnetic calorimeter, Applied Radiation and Isotopes 134 (2018) 395–398. doi:10.1016/j.apradiso.2017.10.042.
URL https://doi.org/10.1016/j.apradiso.2017.10.042